Fractional saturable impurity

Mario I. Molina
Departamento de Física, Facultad de Ciencias, Universidad de Chile, Casilla 653, Santiago, Chile

(Received 7 September 2022; revised 16 November 2022; accepted 28 November 2022; published 7 December 2022)

We examine analytically and numerically the effect of fractionality on a saturable bulk and surface impurity embedded in a one-dimensional lattice. We use a fractional Laplacian introduced previously by us, and by the use of lattice Green functions we are able to obtain the bound state energies and amplitude profiles, as a function of the fractional exponent s and saturable impurity strength χ for both surface and bulk impurity. The transmission is obtained in closed form as a function of s and χ, showing strong deviations from the standard case, at small fractional exponent values. The self-trapping of an initially localized excitation is qualitatively similar for the bulk and surface mode, but in all cases complete confinement is obtained at $s \to 0$, as shown theoretically and observed numerically.

DOI: 10.1103/PhysRevA.106.063504

I. INTRODUCTION

When a defect is inserted in a discrete, periodic system such as a chain of atoms or an optical waveguide array, the original translational symmetry is broken and causes that one of the states detaches from the band and form a localized mode centered at the impurity position. It has been proven that, for one-dimensional (1D) and 2D lattices there is always a localized bound state centered at the defect [1,2], regardless of the strength of the impurity. The rest of the modes remain extended but they are no longer sinusoidal. The single-defect system is the starting point for the study of the more complex system with a finite fraction of disorder, where the main phenomenon of study is Anderson localization [3,4]. Some examples of linear impurities include junction defects between two optical or network arrays [5], coupling defects, discrete networks for routing and switching of discrete optical solitons [6], and also in simple models for magnetic metamaterials, modeled as periodic arrays of split-ring resonators, where magnetic energy can be trapped at impurity positions [7,8].

When nonlinearity is added to a periodic system, mode localization and self-trapping of energy can occur. This localized mode which exists in this nonlinear but otherwise completely periodic system is known as a discrete soliton. In most cases this concentration of energy on a small region increases with the nonlinearity strength and, as a consequence, the nonlinear mode becomes effectively decoupled from the rest of the lattice. In the high nonlinearity limit, the effective nonlinearity is concentrated in a small region around the soliton, and thus, we can consider the rest of the lattice as approximately linear. We are then left with a linear lattice containing a single nonlinear impurity. This simplified system is easier to treat theoretically and closed-form solutions are sometimes possible. In condensed matter, nonlinear impurities appear when one dopes a material with atoms or molecules that have strong local couplings. In optics, the system of interest is a dielectric waveguide array, where one of the guides is judiciously doped with an element with strong polarizability. A more recent example is magnetic metamaterials, where the system is an array of inductively coupled split-ring resonators, where a linear (nonlinear) impurity ring is obtained by, for instance, inserting a linear (nonlinear) dielectric inside its slit to change its resonance frequency. In the absence of the impurity, the modes are extended magnetoinductive plane waves, and when a capacitive impurity is introduced, a localized mode is created. The nonlinear impurity concept has also been explored in studies of embedded solitons [9].

A common approach when dealing with generic impurities is to make an educated guess about the shape of the mode (usually exponential) which then leads to the mode energy and exact spatial profile. However, this procedure might work only partially. For one thing, in the presence of nonlinearity, the number of modes depends on the available energy content, and there is possible bifurcation separating different modes with different stabilities. Also, when boundaries are involved, like impurities close to a surface, the need for a more formal treatment is apparent. An elegant method for dealing with impurity problems is the technique of lattice Green functions [11–13]. Originally devised for linear problems, it has been shown that it can also be extended to nonlinear cases [14–17]. This is the method we will follow in this work, with the added feature of fractionality.

The concept of fractionality has gained considerable interest in recent years. Roughly speaking, it consists of a generalization of the standard derivative of integer order by one of fractional order. It all started with the correspondence between Leibnitz and L'Hopital about possible generalizations of the concept of an integer derivate. The starting point was the calculation of $d^s x^k/dx^s$, for s a real number. This means

$$\frac{d^n x^k}{dx^n} = \frac{\Gamma(k+1)}{\Gamma(k-n+1)} x^{k-n} \to \frac{d^s x^k}{dx^s} = \frac{\Gamma(k+1)}{\Gamma(k-s+1)} x^{k-s}, \tag{1}$$

where $\Gamma(x)$ is the Gamma function. From Eq. (1) the fractional derivative of an analytic function $f(x) = \sum_k a_k x^k$ can be computed by deriving the series term by term. However, this simple procedure is not exempt from ambiguities. These early studies were followed later by rigorous work by several mathematicians including Euler, Laplace, Riemann, and Caputo to name some, and converted fractional calculus from a mathematical curiosity into a research field of its own [18–21]. Several possible definitions for the fractional derivative are known, each one with its own advantages and disadvantages. One of the most common definitions is the Riemann-Liouville form

$$\left(\frac{d^s}{dx^s}\right) f(x) = \frac{1}{\Gamma(1-s)} \frac{d}{dx} \int_0^x \frac{f(s)}{(x-s)^s} ds. \tag{2}$$

Another common form, is the Caputo formula

$$\left(\frac{d^s}{dx^s}\right) f(x) = \frac{1}{\Gamma(1-s)} \int_0^x \frac{f'(s)}{(x-s)^s} ds, \tag{3}$$

where, $0 < s < 1$ is the fractional exponent. This formalism that extends the usual integer calculus to a fractional one, with its definitions of a fractional integral and fractional derivative, has found application in several fields: fractional kinetics and anomalous diffusion [22–24], fluid mechanics [25], strange kinetics [26], Levy processes in quantum mechanics [27], fractional quantum mechanics [28,29], plasmas [30], electrical propagation in cardiac tissue [31], epidemics [32], and biological invasions [33].

In this work we will study the effect of fractionality on the bound state and plane-wave transmission properties of a saturable impurity, seeking to characterize these properties as a function of the fractional exponent s.

II. THE MODEL

.

Let us consider a generic excitation propagating along a 1D chain periodic chain that contains a single saturable impurity at site d:

$$i\,\frac{dC_n}{dt} + V(C_{n+1} + C_{n-1}) + \delta_{n,d}\,\chi\,\frac{C_n}{1+|C_n|^2} = 0, \tag{4}$$

where $C_n(t)$ is the probability amplitude for finding the excitation at site n at time t, V is the hopping parameter, and χ is the nonlinear parameter. In an optical context [34], Eq. (4) describes an array of semiconductor (GaAs/AlGaAs) optical waveguides where one of the guides is doped with a photorefractive element such as lithium niobate doped with a metal: Fe: $LiNbO_3$. The term $V(C_{n+1} + C_{n-1})$ is basically the discrete Laplacian $\Delta_n C_n = C_{n+1} - 2C_n + C_{n-1}$. Then, Eq. (4) can be cast as

$$i\frac{dC_n}{dt} + 2VC_n + V\Delta_n C_n + \delta_{n,d}\,\chi\,\frac{C_n}{1+|C_n|^2} = 0. \tag{5}$$

The next step is to replace the discrete Laplacian Δ_n by its fractional form $(\Delta_n)^s$ in Eq. (5). The form of this fractional discrete Laplacian has been found in closed form, and is given by [35]:

$$(-\Delta_n)^s C_n = \sum_{m\neq n} K^s(n-m)(C_n - C_m), \qquad 0 < s < 1, \tag{6}$$

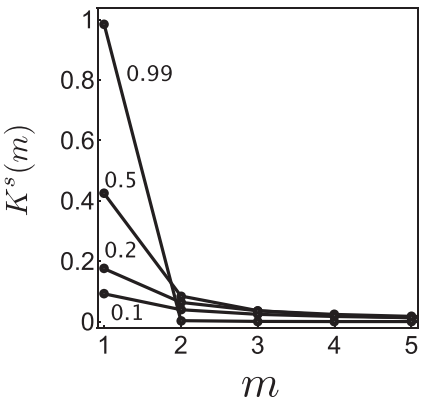

FIG. 1. Decrease of kernel K(m) with distance for several fractional exponents. The numbers labeling each curve denote the fractional exponent.

where

$$K^s(m) = \frac{4^s \Gamma(s+(1/2))}{\sqrt{\pi}|\Gamma(-s)|} \frac{\Gamma(|m|-s)}{\Gamma(|m|+1+s)}, \tag{7}$$

where $\Gamma(n)$ is the Gamma function and s is the fractional exponent. Figure 1 shows $K^s(m)$ as a function of distance m, for several fractional exponents. In all cases we observe a monotonically decreasing behavior. In addition, for each exponent, the maximum value of $K^s(m)$ occurs at $m = 1$ and decreases with s as

$$K^s(1) = \frac{4^s s\,\Gamma(s+(1/2))}{\sqrt{\pi}\,\Gamma(2+s)}. \tag{8}$$

The kernel $K^s(m)$ gives the effective coupling between two sites separated by $|m|$ [10]. By using $\lim_{n\to\infty} \Gamma(n+s) = \Gamma(n)n^s$, one arrives to the asymptotic form $K(m) \to 1/|m|^{1+2s}$, i.e., a power-law decrease of the coupling with distance. For s approaching unity, we have $\lim_{s\to 1^-} K^s(m) = \delta_{m,1}$, while for s near zero, we have $\lim_{s\to 0^+} K^s(m) = s/|m|$. This means that for s near 1 the coupling is mainly between nearest neighbors, and at $s = 1$ the system reduces to the standard one with an integer Laplacian. For s near zero the system becomes long-ranged. We look for stationary modes $C_n(t) = \phi_n\ \exp(i\lambda t)$, obtaining a system of nonlinear difference equations for ϕ_n:

$$(-\lambda + 2V)\,\phi_n + V\sum_{m\neq n} K^s(n-m)(\phi_m - \phi_n) + \delta_{n,d}\,\chi\,\frac{\phi_n}{1+|\phi_n|^2} = 0, \tag{9}$$

where, without loss of generality, the ϕ_n can be chosen as real. Also the $2V$ term in Eq. (9) must be replaced by V when n corresponds to any of the two edge sites, for a finite chain.

In the absence of the saturable impurity, we have solutions of the type $C_n = \phi_n \exp(ikn)$. After inserting this ansatz into Eq. (9), we obtain the dispersion relation

$$\lambda(k) = 2V - 4V\sum_{m=1}^{\infty} K^s(m)\sin((1/2)mk)^2 \tag{10}$$

or, in closed form

$$\lambda(k) = 2V - \frac{16V\ \Gamma(s+(1/2))}{\sqrt{\pi}\ \Gamma(1+s)}(1-\exp(-ik)\ s\ \Gamma(1+s) \times [\ R(1,1-s,2+s;\exp(-ik)) + \exp(2ik) \times R(1,1-s,2+s;\exp(ik))]), \tag{11}$$

where $R(a,b,c;z) = {}_2F_1(a,b,c;z)/\Gamma(c)$ is the regularized hypergeometric function.

Bulk impurity. In the presence of the impurity ($\chi \neq 0$), it becomes easier to compute its properties by using the formalism of the lattice Green function rather than working directly from Eq. (9). In our case the Hamiltonian can be cast as

$$H = H_0 + H_1, \tag{12}$$

$$H_0 = \sum_n \epsilon_n |n\rangle\langle n| + \sum_{n,m} |m\rangle V_{n,m}\langle n|, \tag{13}$$

$$H_1 = \frac{\chi}{1+|\phi_d|^2}|d\rangle\langle d| \tag{14}$$

with

$$\epsilon_n = 2V - V\sum_{m\neq n} K^s(n-m), \tag{15}$$

and

$$V_{nm} = K^s(n-m) = V_{mn}, \tag{16}$$

where the Dirac notation has been used. Hamiltonian H_0 is the unperturbed Hamiltonian, that is, the Hamiltonian in the absence of the impurity, while H_1 is the perturbation due to the presence of the saturable impurity at $n = d$, where for the bulk impurity d is far away from the boundaries of the lattice, while for the surface impurity $d = 0$. The equations of motion for the amplitudes C_n are given by $i\,dC_n/dt = \partial H/\partial C_n^*$. The Green function is defined as the operator

$$G(z) = \frac{1}{z-H}, \tag{17}$$

while we define the unperturbed Green function as

$$G^{(0)}(z) = \frac{1}{z-H_0}. \tag{18}$$

Typically, one has a complete knowledge of H_0 which translates into knowledge of the properties of $G^{(0)}$. This knowledge is used to build G which contains all the information about our system. We formally expand Eq. (17) as a perturbation series in H_1. We start from

$$\begin{aligned} G &= \frac{1}{z-H_0-H_1} = ((z-H_0)-H_1)^{-1} \\ &= [(z-H_0)(1-(z-H_0)^{-1}H_1)]^{-1} \\ &= (1-(z-H_0)^{-1}H_1)^{-1}\ (z-H_0)^{-1} \\ &= (1-G^{(0)}H_1)^{-1}G^{(0)}, \end{aligned} \tag{19}$$

which is nothing else than Dyson's equation [11]. We expand it as

$$G = (1 + G^{(0)}H_1 + G^{(0)}H_1G^{(0)}H_1 + \cdots)\ G^{(0)}, \tag{20}$$

that is,

$$G(z) = G^{(0)} + G^{(0)}\ H_1\ G^{(0)} + G^{(0)}\ H_1\ G^{(0)}\ H_1\ G^{(0)} \cdots . \tag{21}$$

By defining matrix elements $G^{(0)}_{mn} = \langle m|G^{(0)}|n\rangle$, we can write the unperturbed Green function as

$$G^{(0)}_{nm}(z) = \frac{1}{2\pi}\int_{-\pi}^{\pi} \frac{e^{ik(n-m)}dk}{z-\lambda(k)}, \tag{22}$$

where n and m are lattice positions and $\lambda(k)$ is given by Eq. (11). The interesting point here is that due to the particularly simple form of perturbation H_1, we can resum the perturbative series to all orders, in closed form:

$$G(z) = G^{(0)} + \frac{\epsilon}{1-\epsilon\ G^{(0)}_{dd}} G^{(0)}|d\rangle\ \langle d|G^{(0)}, \tag{23}$$

where

$$\epsilon \equiv \frac{\chi}{(1+|\phi_d|^2)}. \tag{24}$$

According to the general theory [11], the energy z_b of the bound state is given by the poles of $G_{dd}(z)$

$$1 = \epsilon\ G^{(0)}_{dd}(z_b) = \chi\frac{G^{(0)}_{dd}(z_b)}{1+\left|\phi^{(b)}_d\right|^2}, \tag{25}$$

while the square of the mode amplitude at site n is given by the residue of $G_{nm}(z)$ at the pole

$$\left|\phi^{(b)}_n\right|^2 = -\frac{G^{(0)^2}_{nd}(z_b)}{G'^{(0)}_{dd}(z_b)}. \tag{26}$$

Also, from general Eqs. (26) and (22), it can be easily proven that the bound state mode is always normalized: $\sum_n |\phi^{(b)}_n|^2 = 1$. The bound state energy equation becomes

$$\frac{1}{\chi} = \frac{G^{(0)}_{dd}(z_b)G'^{(0)}_{dd}(z_b)}{G'^{(0)}_{dd}(z_b) - G^{(0)2}_{dd}(z_b)}. \tag{27}$$

This formalism is also useful to compute the transmission of plane waves across the impurity, The transmission amplitude is given by $T \sim 1/|1-\epsilon G^+_{dd}(z)|^2$, while the reflection amplitude is given by $R \sim \epsilon^2|G^+_{d,d}(z)|^2/|1-\epsilon G^+_{dd}(z)|^2$, with $G^+(z) = \lim_{\eta\to 0}\ G(z+i\eta)$ and ϵ given by Eq. (24). After normalizing these amplitudes by $N = T + R$ the transmission coefficient t and reflection coefficient r can be expressed as

$$t(z) = \frac{1}{1+\epsilon^2\left|G^+_{dd}(z)\right|^2}, \tag{28}$$

$$r(z) = \frac{\epsilon^2\left|G^+_{dd}(z)\right|^2}{1+\epsilon^2\left|G^+_{dd}(z)\right|^2}, \tag{29}$$

and z is inside the band $\lambda(k)$. Since the transmission coefficient is also equal to the probability at the impurity site, $\epsilon = \chi/(1+t)$, Eq. (28) becomes a cubic equation for t:

$$(1+t)^2 - t(b+(1+t)^2) = 0 \quad \text{with} \quad b \equiv \chi^2\left|G^+_{dd}(z)\right|^2 \tag{30}$$

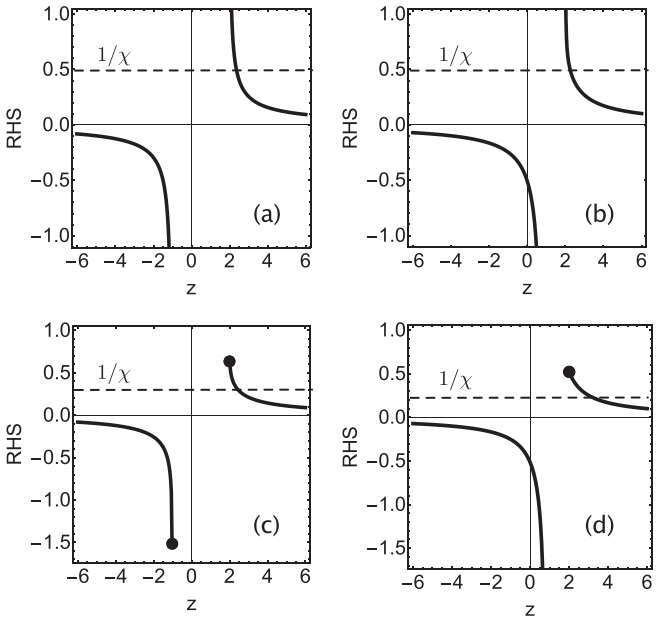

FIG. 2. Bound state condition [Eq. (27)] for the bulk impurity (a) $s = 0.8$ and (b) $s = 0.2$, and the surface impurity (c)$s = 0.8$ and (d)$s = 0.2$. For the surface impurity, the dots denotes the value of the RHS at the band edges. The intersection of the horizontal line with the RHS gives the bound state energy.

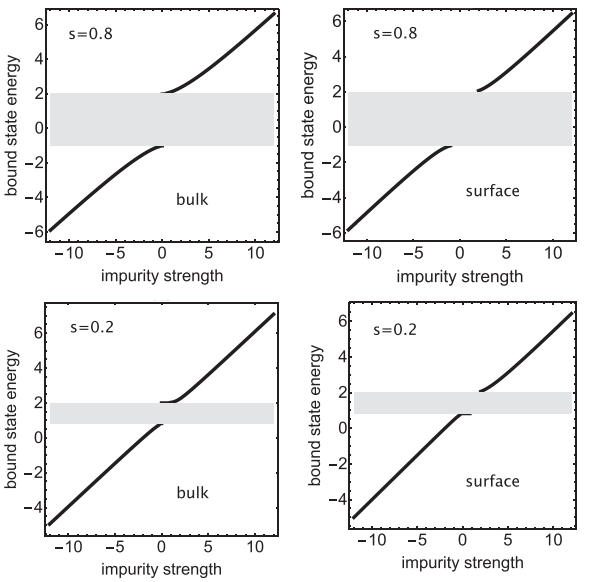

FIG. 3. Bound state energy versus impurity strength for the bulk and surface impurity cases, and for a couple of different fractional impurities s.

with real solution

$$t = \frac{1}{3}\Bigg(-1 - \frac{2^{1/3}(-4+3b)}{(16+9b+\sqrt{27b\,(32+b(-13+4b))})^{1/3}} + 2^{-1/3}\big(16+9b+\sqrt{27b\,(32+b(-13+4b))}\,\big)^{1/3}\Bigg). \tag{31}$$

Fractionality is implicit in Eq. (31) through b which depends on G^{+} which, in turn, depends on $\lambda(k)$ through Eq. (11).

Surface impurity. In the case of the surface impurity, located at $n = 0$, we have to take into account the presence of the boundary. That is, since there is no lattice to the left of $n = 0$, $G^{(0)}_{mn}$ should vanish identically at $n = -1$. Thus, $G^{(0)}_{mn} = G^{\infty}_{mn} - G^{\infty}_{m,-n-2}$ where G^{∞}_{mn} is the unperturbed Green function for the infinite lattice. Using the representation (22), we have

$$G^{(0)}_{mn} = \frac{1}{2\pi}\int_{-\pi}^{\pi}\frac{e^{ik(m-n)}}{z-\lambda(k)} - \frac{1}{2\pi}\int_{-\pi}^{\pi}\frac{e^{ik(m+n+2)}}{z-\lambda(k)}. \tag{32}$$

The computation of the bound state energy and bound state amplitude proceed as before, using this new $G^{(0)}_{mn}$ (32), extracted from the method of images.

III. RESULTS

.

We begin by taking a look at the bound state energy equation (27). Figure 2 shows the RHS of Eq. (27) as a function of the frequency z. The horizontal dashed line represents the value of some $1/\chi$, whose intersection with the RHS curve give us the bound state energy. For the bulk case, the RHS curve diverges at the edges of the band and there is a single bound state solution for any χ. Also, as the fractional exponent is decreased, the lower band edge shrinks causing the negative energy eigenvalue to shift towards less negative values. For the surface impurity case, the situation is similar to the bulk case, except that now the RHS of Eq. (27) does not diverge at the band edges, which means that a minimum χ value must be reached in order for an intersection with $1/\chi$ to occur. The behavior with a change in fractional exponent s is similar to the bulk case. Figure 3 shows the bulk and surface bound state energies as a function of the impurity strength for several fractional exponents. In all cases there is a single bound state mode that lives outside the bands, whose width decreases with a decrease en s. The bandwidth is given by $\lambda(0) - \lambda(\pi)$, where $\lambda(k)$ is given by Eq. (11). In the limit of large impurity strength, it is possible to obtain the asymptotic value for z_b: Since z_b is monotonic with χ, we have that $G^{(0)}_{00}(z_b) \to 1/z_b$, $G'^{(0)}_{00}(z_b) \to 1/z_b^2$. After replacing this into the bound state energy equation (27), we obtain $z_b \to \chi/2$ and $|\phi_n|^2 \to \delta_{n,d}$, i.e., complete localization at the impurity site. We notice that the phenomenology is, in general, similar to the case of a linear impurity [36]. This could be explained by the nature of the saturable nonlinearity where one could express the nonlinearity as $\chi_{\text{eff}} = \chi/(1+|\phi_d|^2) < \chi$. Thus, the saturable impurity is always "weaker" than the linear one.

Figure 4 shows some bulk and surface bound state profiles for several values of the impurity strengths and fractional exponents. They look similar to the localized modes of cubic impurities. However, while for the standard case ($s \approx 1$) the change $\chi \to -\chi$ produces an staggered version of the mode, $\phi_n \to (-1)^n\phi_n$, here for $s < 1$ this symmetry is debilitated, specially at low s values where the staggered mode is lost completely. Same happens for the surface bound state.

Figure 5 shows the transmission of plane waves across the saturable impurity, as a function of energy. We use the exact

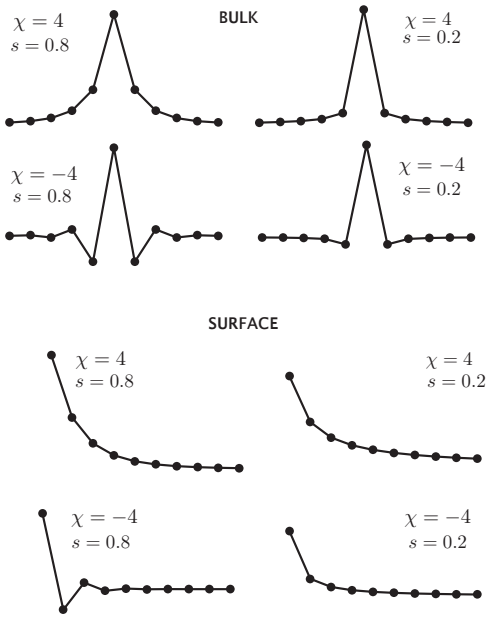

FIG. 4. Bulk and surface bound state profiles for some impurity strengths and fractional exponents.

expression Eq. (31). For each fractional exponent s, we plot curves corresponding to different impurity strengths χ. The first thing we notice is that, as s decreases, the energy range for transmission shrinks. This is due to the reduction of the bandwidth with s and was already observed in Fig. 3. On the other hand, for each fixed s, the transmission decreases with increasing χ, as expected. It can also be proved that there are no resonances ($t = 1$): If we set $t = 1$ in Eq. (30), we obtain the condition $b = 0$. However, $b = \chi^2 |G_{00}^{+}|^2 > 0$, so there is no resonance except in the limit of no impurity. Finally, let us

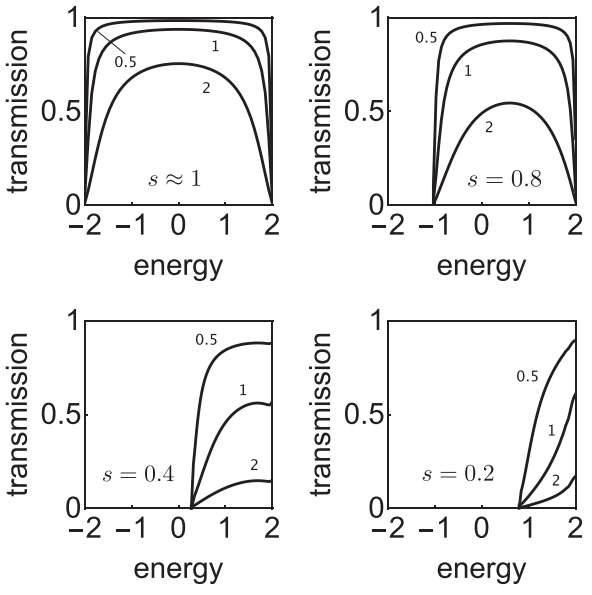

FIG. 5. Transmission of plane waves across the saturable impurity, for different fractional exponents s and different impurity strengths χ labeling each curve.

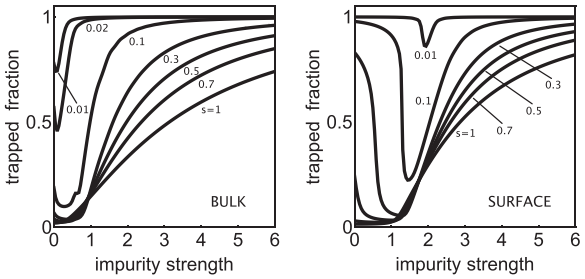

FIG. 6. Time-averaged trapped fraction at impurity site versus nonlinearity strength for several fractional exponents s, for the bulk and surface impurity. The numbers labeling each curve represent the fractional exponents ($N = 233$, $Vt_{\max} = 60$, time step was allocated by an adaptive time step method).

consider the issue of self-trapping. We put an initial excitation on the impurity site and observe its dynamical evolution at long times. When there is a finite portion remaining on the impurity site, we speak of selftrapping. This type of self-trapping is a common feature of many discrete nonlinear lattices for a variety of nonlinearity types. Figure 6 shows the self-trapping for the bulk and surface impurity, and for several values of the fractional impurity s. Roughly speaking both cases are qualitatively similar, with an amount of trapped fraction that increases with a decrease in s. A very distinctive feature of Fig. 6 is the presence, in both cases, of self-trapping at small value of χ. This linear trapping increases with a decrease in s and at $s \to 0$, the trapped fraction approaches unity, independent of the impurity strength. This behavior can be explained as follows: When $s \to 0$, $K^s(m) \to (s/m) + \mathcal{O}(s^2)$. Thus, evolution equation (5) reduces to

$$i\frac{dC_n}{dt} + 2VC_n + \delta_{n,d}\,\chi\,\frac{C_n}{1+|C_n|^2} = 0 \tag{33}$$

with initial condition $C_n(0) = \delta_{nd}$, where $d = 0$ for the surface impurity, or $d \sim N/2$ for the bulk impurity. To verify this further, the computed the time evolution of Eq. (5) including the Laplacian term $\sum_{m\neq n} K^s(n-m)\,(C_n(t) - C_m(t))$. We observe that, as s approaches zero, the contribution of the Laplacian term goes to zero and thus, Eq. (33) is correct. After multiplying Eq. (33) by C_n^*, we have

$$iC_n^*\frac{dC_n}{dt} + 2V|C_n|^2 + \delta_{n,d}\,\chi\,\frac{|C_n|^2}{1+|C_n|^2} = 0. \tag{34}$$

Finally, we substract from Eq. (34) its complex conjugate, obtaining

$$\frac{d}{dt}|C_n|^2 = 0, \tag{35}$$

which implies $C_n(t) = C_n(0) = \delta_{nd}$. Thus, at $s \to 0$ there is complete trapping of the initial excitation, regardless of the impurity strength χ. This is clearly seen in Fig. 6. For finite s, the trapping curves show that for the surface case more impurity strength is needed to effect a similar trapped value as in the bulk case. Perhaps this is a manifestation of a sort of a position uncertainty effect: The presence of a surface confines the impurity much more than in the bulk case, thus increasing its kinetic energy; thus the need for a stronger potential well χ to effect trapping.

IV. CONCLUSIONS

We have examined analytically and numerically the physics of a single saturable impurity embedded in a 1D lattice, when the usual discrete Laplacian is replaced by a fractional one, characterized by a fractional exponent. We considered two types of impurity: a bulk one, located far away from the edges of the lattice, and a surface impurity located at one of the edges (site zero). By means of the formalism of lattice Green functions, we determined the existence of a single bound state. While for the bulk case there is a bound state for any amount of impurity strength, for the surface case a minimum amount of impurity strength is needed. These features are markedly different from the well-known case of a cubic impurity [15,37]. There, for the bulk case a bound state is only possible for impurity strengths larger than a critical value, while a surface impurity also requires a minimum impurity strength to generate a bound state, and up to two bound states are possible. Rather, our results resemble the ones for the linear impurity. The fractional exponent does not seem to play an important role in this respect.

The bound state energy curves are more or less similar for the bulk and surface cases, for given values of the fractional exponent. When this value is close to unity (standard case), the bound state spatial profiles resemble the ones found for the cubic impurity where the staggered-unstaggered symmetry is obeyed. However as the exponent approaches zero, this symmetry is no longer obeyed.

The transmission of plane waves across the impurity decreases in an overall sense, since the energy interval of the passing waves shrinks with a decrease of the fractional exponent. In fact, in the limit of a vanishing exponent, the only wave that can be transmitted is the one with energy equal to 2.

The self-trapping of an initially localized excitation is not dissimilar for the bulk and surface cases. In both cases it increases monotonically with an increase in impurity strength and, for a fixed impurity strength, it increases with a decreasing fractional exponent. The main difference between the two cases is that for the surface case, it takes more impurity strength to effect a degree of trapping. For both cases we observe the existence of linear trapping at small impurity strength, for all fractional exponents. In the limit of a vanishing exponent, the trapped fraction converges to unity, regardless of the impurity strength value. This can be traced back to the vanishing of the effective coupling $K^s(m)$ at small fractional exponents.

All in all, the main effect of fractionality in this saturable impurity was rather secondary, except at small values of the fractional impurity. This is the regime where the bandwidth is substantially shrunk, pushing all eigenvalues together and thus, inducing a tendency towards degeneration.

ACKNOWLEDGMENT

This work was supported by Fondecyt Grant No. 1200120.

[1] J. C. Slater and G. F. Koster, Simplified LCAO method for the periodic potential problem, Phys. Rev. **94**, 1498 (1954).
[2] W. A. Harrison, *Electronic Structure and the Properties of Solids* (Freeman, San Francisco, CA, 1980).
[3] E. N. Economou and C. M. Soukoulis, Connection of localization with the problem of the bound state in a potential well, Phys. Rev. B **28**, 1093 (1983).
[4] E. N. Economou, C. M. Soukoulis, and A. D. Zdetsis, Localized states in disordered systems as bound states in potential wells, Phys. Rev. B **30**, 1686 (1984).
[5] A. E. Miroshnichenko, M. I. Molina, and Y. S. Kivshar, Localized modes and bistable scattering in nonlinear network junctions, Phys. Rev. E **75**, 046602 (2007).
[6] D. N. Christodoulides and E. D. Eugenieva, Blocking and Routing Discrete Solitons in Two-Dimensional Networks of Nonlinear Waveguide Arrays, Phys. Rev. Lett. **87**, 233901 (2001).
[7] B. Wang, J. Zhou, T. Koschny, and C. M. Soukoulis, Nonlinear properties of split-ring resonators, Opt. Express **16**, 16058 (2008).
[8] M. I. Molina, Defect modes, Fano resonances and embedded states in magnetic metamaterials, in *Spontaneous Symmetry Breaking, Self-Trapping, and Josephson Oscillations*, edited by B. A. Malomed (Springer-Verlag, Berlin, 2013).
[9] K. Yagasaki, A. R. Champneys, and B. A. Malomed, Discrete embedded solitons, Nonlinearity **18**, 2591 (2005).
[10] M. I. Molina, The fractional discrete nonlinear Schrödinger equation, Phys. Lett. A **384**, 126180 (2020).
[11] E. Economou, *Green's Functions in Quantum Physics* (Springer-Verlag, Berlin, 1983).
[12] G. Barton, Elements of Green's Functions and Propagation: Potentials, Diffusion, and Waves (Oxford University Press, Oxford, UK, 1989).
[13] D. G. Duffy, *Green's Functions with Applications* (CRC Press, Boca Raton, 2001).
[14] M. I. Molina, Nonlinear impurity in a square lattice, Phys. Rev. B **60**, 2276 (1999).
[15] M. I. Molina, Nonlinear surface impurity in a semi-infinite lattice, Phys. Rev. B **71**, 035404 (2005).
[16] M. I. Molina, Nonlinear surface impurity in a semi-infinite two-dimensional square lattice: Green function approach, Phys. Rev. B **74**, 045412 (2006).
[17] M. I. Molina, Interaction of a discrete soliton with a surface mode, Phys. Rev. B **73**, 014204 (2006).
[18] R. Hermann, *Fractional Calculus -An Introduction for Physicists* (World Scientific, Singapore, 2014).
[19] B. West, M. Bologna, and P. Grigolini, *Physics of Fractal Operators* (Springer, New York, 2003).
[20] K. S. Miller and B. Ross, *An Introduction to the Fractional Calculus and Fractional Differential Equations* (Wiley, New York, 1993).
[21] R. Hilfer (Ed.), *Applications of Fractional Calculus in Physics* (World Scientific, Singapore, 2000).

[22] R. Metzler and J. Klafter, The random walk's guide to anomalous diffusion: A fractional dynamics approach, Phys. Rep. **339**, 1 (2000).

[23] I. M. Sokolov, J. Klafter, and A. Blumen, Fractional kinetics, Phys. Today **55**(11), 48 (2002).

[24] G. M. Zaslavsky, Chaos, fractional kinetics, and anomalous transport, Phys. Rep. **371**, 461 (2002).

[25] L. A. Caffarelli and A. Vasseur, Drift diffusion equations with fractional diffusion and the quasigeostrophic equation, Ann. Math. **171**, 1903 (2010).

[26] M. F. Shlesinger, G. M. Zaslavsky, and J. Klafter, Strange kinetics, Nature (London) **363**, 31 (1993).

[27] N. Cufaro Petroni and M. Pusterla, Levy processes and Schrödinger equation, Physica A **388**, 824 (2009).

[28] N. Laskin, Fractional quantum mechanics, Phys. Rev. E **62**, 3135 (2000).

[29] N. Laskin, Fractional Schödinger equation, Phys. Rev. E **66**, 056108 (2002).

[30] M. Allen, A fractional free boundary problem related to a plasma problem, Commun. Anal. Geom. **27**, 1665 (2019).

[31] A. Bueno-Orovio, D. Kay, V. Grau, B. Rodriguez and K. Burrage, Fractional diffusion models of cardiac electrical propagation: role of structural heterogeneity in dispersion of repolarization, J. R. Soc., Interface **11**, 20140352 (2014).

[32] A. Atangana, Application of Fractional Calculus to Epidemiology, in *Fractional Dynamics*, edited by C. Cattani, H. M. Srivastava, and X.-J. Yang (De Gruyter Open, Poland, 2015).

[33] H. Berestycki, J.-M. Roquejoffre and L. Rossi, The influence of a line with fast diffusion on Fisher-KPP propagation, J. Math. Biol. **66**, 743 (2013).

[34] M. Stepić, E. Smirnov, C. E. Rüter, L. Prönneke, D. Kip, and V. Shandarov, Beam interactions in one-dimensional saturable waveguide arrays, Phys. Rev. E **74**, 046614 (2006).

[35] O. Ciaurri, L. Roncal, P. R. Stinga, J. L. Torrea, J. L. Varona, Nonlocal discrete diffusion equations and the fractional discrete Laplacian, regularity and applications, Adv. Math. **330**, 688 (2018).

[36] M. I. Molina, Saturable impurity in an optical array: Green function approach, Phys. Rev. E **98**, 032206 (2018).

[37] G. P. Tsironis, M. I. Molina, and D. Hennig, Generalized nonlinear impurity in a linear lattice, Phys. Rev. E **50**, 2365 (1994).